The Journal of the Korean Society of
Coastal and Ocean Engineers
Vol. 7, No. 3, pp. 277~288, September 1995

A Model for Vertical Transport of Fine Sediment and Bed Erodibility in a Wave-Dominated Environment

波浪支配環境에서의 微細堆積物 垂直移動에 관한 模型

Kyu Nam Hwang*
황 규 남*

Abstract [ ] Prediction of turbidity due to fine-grained bed material load under wave action is critical to any assessment of anthropogenic impact on the coastal or lacustrine environment. Waves tend to loosen mud deposits and generate steep suspension concentration gradients, such that the sediment load near the bottom is typically orders of magnitude higher than that near the surface. In a physically realistic but simplified manner, a simple mass conservation principle has been used to simulate the evolution of fine sediment concentration profiles and corresponding erodible bed depths under progressive, nonbreaking wave action over mud deposits. Prior field observations support the simulated trends, which reveal the genesis of a near-bed, high concentration fluidized mud layer coupled with very low surficial sediment concentrations. It is concluded that estimation of the depth of bottom erosion requires an understanding of mud dynamics and competent *in situ* sediment concentration profiling. Measurement of sediment concentration at the surface alone, without regard to the near-bed zone, can lead to gross underestimation of the erodible bed depth.

要 旨 : 파랑운동하에서 미세한 해저물질로 인한 混濁度 예측은 해안 또는 湖沼環境에 인간이 끼친 영향을 평가하는데 있어서 중요하다. 파랑은 泥土의 퇴적작용을 완화하고 급격한 부유농도구배를 형성하려는 경향이 있어 해저면 가까이의 퇴적물에 미치는 부하가 대체로 해수면 가까이의 것보다 크다. 물리적으로 실질적이나 단순화된 방법으로 질량보존법칙이 미세입자의 농도분포 진척과 비쇄파 진행파의 작용하에서 해저면 진흙층의 침식에 상당하는 깊이를 모의하는데 사용되어 왔다. 앞서의 현장관측은 해저면 근처의 모의된 경향을 보여주고 있는데 그 특성은 농도가 크면 매우 적은 표층토사와 결합되어 진흙층을 액상화시킨다. 결론적으로 해저면 침식 깊이의 예측은 泥水力學의 이해와 충분한 현장에서의 토사농도단면측정이 요구된다. 해저면을 무시한 해수면 토사농도만의 측정은 해저면 침식 깊이의 총체적인 과소평가를 유발할 수 있다.

1. INTRODUCTION

The need to predict the turbidity in water due to fine-grained sediment suspension under wave action over mud deposits is well known. In particular, predictions of sediment concentration profiles are critical to sedimentation, erosion, and sorbed contaminant transport studies. Fine sediment particles can be easily transported by hydrodynamic flows such as waves and currents. The presence of these particles in the water column affects acoustic transmission, heat absorption and the depth of the eutrophic zone (Luettich *et al.*, 1989). Because these sediments also have a strong affinity for sorbing nutrients and toxic chemicals, sediments which have been deposited on the bottom may function as a source of contaminants to the water column if they are disturbed by eroding forces resulting, for instance, from wave action. An outstanding example of a water body experiencing these problems is Lake Okeechobee, the largest shallow lake in Florida. This lake shows typical signs of artificial eutrophi-

*노스캐롤라이나 주립대학교 토목공학과 (Department of Civil Engineering, North Carolina State University, P.O. Box 7908, Raleigh, NC 27695-7908)

cation mainly due to increased phosphorus loading associated with the surrounding region.

The transport processes of fine sediments are particularly important in a wave dominated environment (e.g., in shallow lakes and estuaries), since sediments may repeatedly settle to the bottom and be resuspended throughout the water column by periodic forces such as astronomical tides or by episodic forces such as storm events. The accurate prediction of fine sediment transport, which is typically performed through numerical solutions of the sediment mass transport equation, is strongly contingent upon an understanding of the structure of the vertical profile of sediment concentration and interaction of this profile with the flow field. However, modeling of fine sediment transport is limited by the knowledge of physical mechanisms relating the response of mud beds to wave action. Waves tend to loosen the mud deposit and generate steep suspension concentration gradients, making the sediment load near the bottom typically orders of magnitude higher than that near the surface. Neglecting this characteristic of sediment concentration profiles under wave action can therefore lead to significant errors in calculating the associated flux of sediment mass and consequently in estimating the erodibility of mud deposits.

The issue of turbidity generation is examined here in the context of the response of muddy sediment deposits to eroding forces resulting from non-breaking, progressive waves. While turbidity can arise from a number of sources, the focus here is on fine-grained bed material load, which implies suspended sediment related to bed erosion and deposition. It is therefore instructive to consider fine sediment erosion and deposition under waves in a physically realistic, albeit simplified, manner so as to simulate field-observed trends in concentration profile evolution. As shown later in this paper, this type of analysis leads to observations concerning erodible depths in muddy deposits and guidelines for field measurement procedures.

2. VERTICAL STRUCTURE OF SUSPENSION UNDER WAVES

A representative illustration of suspension concentration profile evolution by wave action over coastal mud flats is shown in Fig. 1, using data presented by Kemp and Wells (1987). Four instantaneous (turbulence-mean) vertical concentration profiles for suspended sediment are included in figure 1. Profiles B and C represent sediment concentration profiles during the passage of a winter cold front, while profiles A and D represent pre-frontal and post-frontal conditions, respectively. The data were obtained over a three day period at a site on the eastern margin of the Louisiana chernier plain where the tidal range is less than 0.5 m. Wave height during front passage was on the order of 13 cm and wave period was 7 sec. Of particular interest is the development of a near-bed, high concentration suspension layer by the frontal wind-generated waves (profiles B and C), which was previously absent (profile A). The post-frontal profile D further suggests that this layer may have persisted following the front, conceivably due to the typically low rate at which such a layer dewaters. The suspension concentration in the upper water column was higher following the front than during the front, possibly due to sediment advection from a neighboring area of higher turbidity.

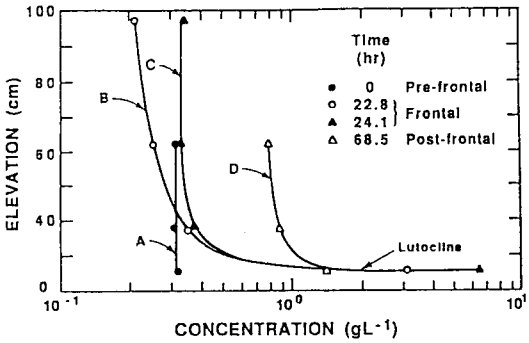

Fig. 1. Vertical suspended sediment profiles obtained before, during and after the passage of a winter cold front at a wave-dominated coastal site in Louisiana. (adapted from Kemp and Wells, 1987).

Concentration profiles qualitatively similar to those shown in Fig. 1 have been reproduced in laboratory flume tests involving wave action over soft muddy deposits (Ross, 1988). Near the bottom a rapidly saturated fluid mud layer develops with the occurrence of a persistent lutocline. The eleva-

tion of the stabilized lutocline is largely determined by a balance between the rate of turbulent kinetic energy input and the buoyancy flux determined by the sediment settling rate. Diffusion due to the wave field is characteristically slow above the lutocline in the water column, so that the concentration there increases to modest levels only. It follows that surface concentrations are not necessarily representative of what occurs at the bottom.

The formation of a high concentration fluidized layer of sediment at the bottom is characteristic of wave-influenced environments. The presence of such a layer with a marked lutocline is not restricted to estuaries and coastal waters, but can also exist in fresh water lakes (Wolanski et al., 1989). In lakes such layers are episodically generated, but due to relatively low rates of dewatering, they may be more common and persistent than previously thought. Gleason and Stone (1975) measured sediment concentration at the water surface during a storm event in the southern part of Lake Okeechobee, Florida. By assuming the entire 4.6 m water column had a vertically uniform concentration (based on a measured surface value) of 102 mg/L, they reported an erodible bed thickness of 2.3 mm (see Fig. 2) which seems unrealistically small. However, on the basis of an examination of bottom cores from the same lake they concluded that a "fluid zone" comprised of a sediment layer of thickness 7-20 cm probably occurs near the bed in this lake. Since fluidized mud is easily entrained by waves (Maa and Mehta, 1987), it is essential to determine the erodible bed thickness by considering the sediment erosion/deposition caused by wave-induced bottom stress.

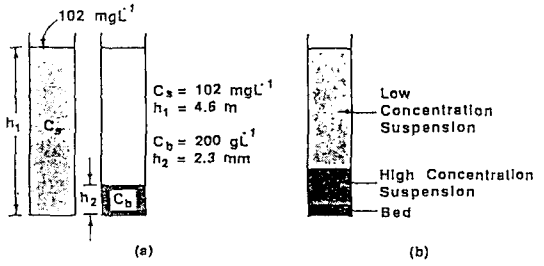

Fig. 2. a) Relationship between uniform suspension concentration, C_s, in water column of depth h_1, and the corresponding thickness, h_2, of bed of concentration C_b; b) High concentration suspension layer between low concentration suspension and bed.

3. APPROACH TO MODELING OF VERTICAL TRANSPORT DYNAMICS

3.1 Governing Equation

The temporal and spatial variations of suspended sediment concentration in the water column subjected to wave action are governed by the mass conservation equation. By considering a differential control volume and equating the time rate of sediment accumulation inside the volume to the net flux of sediment through its boundaries, the mass conservation equation for suspended sediment concentration can be written in the Cartesian coordinates (x, longitudinal: y, lateral: and z, vertical positive downwards from the water surface) as

$$\frac{\partial C}{\partial t} = -\nabla \cdot \boldsymbol{F} \tag{1}$$

where C (x, y, z, t) is the instantaneous sediment concentration (mass of sediment/volume of suspension) and $\boldsymbol{F}$ is the sediment flux vector. No decay term is of course needed in this equation since suspended sediment mass can be assumed to be conserved. The flux, $\boldsymbol{F}$, arises from fluid motion, molecular diffusion and sediment settling. Since turbulent diffusivity is much greater than molecular diffusivity, the terms corresponding to the latter are usually neglected (McCutcheon, 1983).

Since the present analysis is concerned with the vertical structure of sediment concentration, only the vertical transport terms are of interest. In fact, Ross (1988) shows through non-dimensional scaling that in a typical coastal settling the horizontal and vertical advection terms and horizontal diffusion terms can be neglected in a simplified analysis. This allows Equation 1 to be reduced to

$$\frac{\partial C}{\partial t} = -\frac{\partial}{\partial z}(F_d + F_s) \tag{2}$$

Eq. (2) illustrates that the temporal changes in concentration are affected by the vertical gradients in the gravitational settling flux, F_s, and the upward diffusive flux, F_d. Since advective effects have been

neglected in this equation, the treatment inherently becomes somewhat restrictive as a result. However, it is advantageous to highlight the role of vertical mass fluxes in simulating wave-induced turbidity.

The upward diffusive flux, Fd, is expressed as

$$F_d = -K_z \frac{\partial C}{\partial z} \tag{3}$$

where K_z is the vertical mass diffusivity. For sediment in suspension the vertical diffusivity, K_z, is a function of concentration gradient ($\partial C/\partial z$), because there is diffusion damping associated with density gradient due to negative buoyancy. Due to this fact the diffusive flux is highly nonlinear in concentration gradient dependence. The settling flux, F_s, is expressed as

$$F_s = W_s C \tag{4}$$

where the settling velocity, W_s, is in general a function of concentration. Therefore, the settling flux is also non-linear in concentration dependence.

Boundary conditions at the water surface and sediment bed must be defined for the solution of Eq. (2). At the water surface ($z=0$), the net zero flux condition is applied so that $F=F_s+F_d=0$. This means there is no net transport across the free surface and, therefore, diffusion flux always counterbalances the settling flux. At the sediment bed ($z=z_b$), it is essential to define a bed flux term, F_b (mass of sediment per unit bed area per unit time) as concerns erosion (F_e) and deposition (F_p) fluxes. For example, at the bed $F_d=F_e$ during erosional event and $F_s=F_p$ during deposition. The magnitudes of F_e and F_p are typically based on bed shear stresses relative to threshold erosion and deposition shear stress values, respectively. It is evident then that the characteristics of the concentration profile are quite sensitive to the time histories of erosion and deposition, since these represent the source or sink to the total mass in suspension. For example, if the bed erosion flux exceeds the entrainment rate of the near bottom, high concentration layer into the upper water column, a fluidized mud layer would form.

3.2 Bed Fluxes

The bed fluxes are the overall source and sink components of sediment mass in the evolution of the vertical suspension profile, corresponding to the deposition flux, F_p, and the erosion flux, F_e. In the natural environment, it is often difficult to separately identify the phases of the deposition and those of the erosion as a consequence of the time-dependent nature of the flow field. For the purpose of mathematical modeling, however, deposition and erosion of fine cohesive sediment must be provided as separate, bed shear stress dependent, relationships.

Expression for the erosion flux for erosion under wave action (Maa, 1986) is given as

$$F_e = \frac{\partial m}{\partial t} = \varepsilon_M \left(\frac{\tau_b - \tau_s}{\tau_s} \right) \tag{5}$$

where m is the suspended sediment mass per unit bed area, τ_b is the bed shear stress, τ_s is the critical bed shear strength for erosion, and ε_M is the erosion rate when $\tau_b = 2\tau_s$. Since shear strength of a uniform bed does not vary with depth, the erosion flux (F_e) remains constant, represented by ε_M, under a constant τ_b. In general, both τ_s and ε_M depend on the sedimentary composition and bed density, and need to be determined from laboratory tests in which beds of different densities of the given sediment are eroded at different applied stresses.

Fig. 3 shows an example of the type of erosion rate-bed shear stress relationship obtained with muddy sediment from Lake Okeechobee (Hwang, 1989). The bulk density (ρ_B) was 1.10 g/cm^3. The fine-grained sediment was rich in organics (40% by weight), and the predominant clay in the sediment was kaolinite, together with sepiolite and montmorillonite. For such a sediment the mud-water interface is usually ill-defined even under quiescent conditions; a relatively thin "fluff" layer of largely organic aggregates of practically no shear strength overlies stronger material below. The outcome is two distinct erosion rate lines, with the initial one corresponding to practically no shear strength. The second steeper line, essentially representing be erosion, corresponds to $\tau_s = 0.43$ N/m^2 (obtained by extrapolation) and $\varepsilon_M = 2.82$ mg/cm^2/hr in conformity with Eq. (5). With increasing bed density τ_s increases while ε_M decrea-

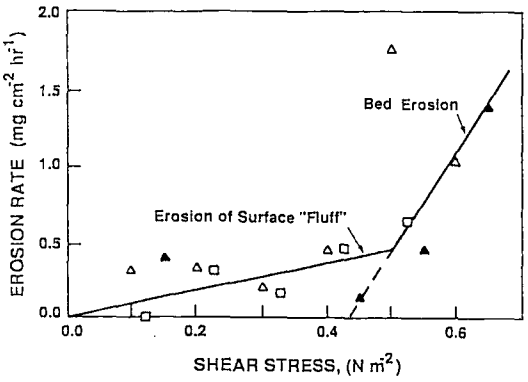

Fig. 3. An illustrative erosion rate relationship obtained in laboratory flume experiment using mud and fluid from Lake Okeechobee.

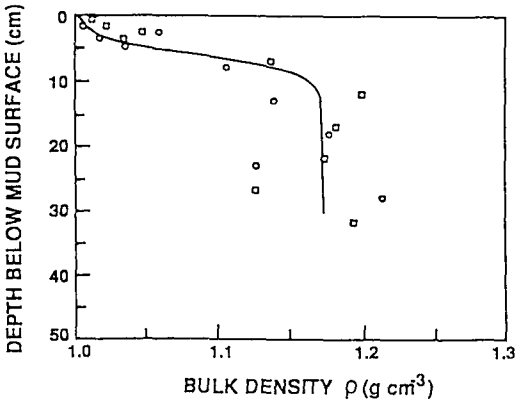

Fig. 4. Typical bulk density variation of the bottom mud layer with depth in Lake Okeechobee.

ses. Experimental data such as those in Fig. 3 (ignoring the relatively minor contribution from fluff erosion) were used to obtain relationships of the form;

$$\tau_s = a_s(\rho_B - \rho_f)^{b_s} + c_s \tag{6}$$

and

$$\ln \varepsilon_M = s_1 \exp\frac{s_2}{\rho_B - \rho_3} \tag{7}$$

where $a_s=0.88$, $b_s=0.2$, $\rho_f=1.065$ g/cm^3, $s_1=0.23$, $s_2=0.198$ and $\rho_3=1.002$ g/cm^3.

Depth-varying density is characteristic of muddy deposits. The profile shown in Fig. 4 is illustrative of bulk density profiles found at the bottom of Lake Okeechobee. The density increased relatively rapidly in the top ~10 cm followed by a more or less uniform substrate approaching 1.2 g/cm^3. Assuming a uniform bottom sediment density or concentration is therefore unrealistic particularly in the top few centimeters. In fact, as a consequence of the dependence to τ_s and ε_M on ρ_B, the rate at which the bed will scour under a constant applied stress will decrease with time until at some depth $\tau_b=\tau_s$, when erosion will cease.

It is essential to point out that erosion rate expressions of the form of Eq. (5) are only applicable to comparatively dense beds having measurable strength. At low bulk densities there is practically no effective stress in the sediment-fluid mixture, and the mud is essentially a fluid (Sills and Elder, 1986). Entrainment of fluid mud is dependent on a representative Richardson number accounting for density stratification between the fluid layer and overlying water (Odd and Rodger, 1986; Srinivas, 1989). Recognizing, however, that for the demonstrative purpose at hand, since the use of an entrainment function different from Eq. (5) for the fluid portion of the bottom deposit would not generate materially different results, at least in the qualitative sense, Eq. (5) is assumed to be applicable to the entire deposit below the mud-water interface defined under quiescent (no-wave) initial condition, i.e. when all sediment is settled with clear water above. For future reference, however, it is worth bearing in mind the limitations of using Eq. (5) in fluidized mud environments.

The rate of deposition, F_p, is obtained from (Mehta, 1988a)

$$F_p = \frac{\partial m}{\partial t} = -pW_sC \tag{8}$$

where p is defined as the probability of deposition, and C is the near-bed suspended sediment concentration. The probability of deposition, p, is described by

$$p = H\left(1 - \frac{\tau_b}{\tau_c}\right) \tag{9}$$

where τ_c is a critical shear stress for deposition and H is a heavyside function represented as $H=1$ when $\tau_b<\tau_c$ and $H=0$ when $\tau_b>\tau_c$. A typical value

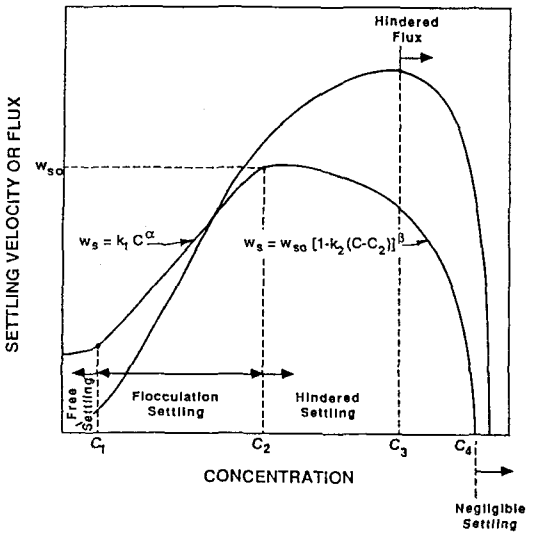

Fig. 5. A schematic description of settling velocity variation with suspension concentration of fine-grained sediment.

for τ_c is considered to be 0.1 N/m^2 (Mehta, 1988a). The settling velocity, W_s, is the critically important parameter in specifying F_p, and is discussed further later.

3.3 Settling Velocity

The settling velocity of cohesive sediment strongly varies with concentration in suspension. Moreover, the settling velocity is a function of the suspension and not exclusively of the sediment (Mehta, 1988b). Fig. 5 is a descriptive plot of the relationship which may typically be found between the settling velocity, W_s, and the suspended sediment concentration, C. Also shown is the variation of the corresponding settling flux, $F_s=W_s$ C. The settling velocity regime can be conveniently divided into three sub-ranges depending upon the concentration. These are identified as free settling, flocculation settling and hindered settling.

Free settling occurs in the range of C less than C_1 as identified in Figure 5. In this range the particles or aggregates settle independently without mutual interference and the settling velocity no longer depends on concentration. It is also noteworthy that very small particles of less than ~1 μm size are influenced by Brownian motion and do not settle early. For such particles Ws must be corrected for by concentration from Brownian diffusion (Lick, 1982). For cohesive sediments, the upper concentration limit, C_1, is considered to be in the range of 0.1 to 0.3 g/L (Mehta, 1988b).

Between concentrations C_1 and C_2, identified as the flocculation settling range, increasing concentration leads to increasing interparticle collision and consequently enhanced aggregation. This in turn means that the settling velocity increases with concentration due to the formation of stronger, denser and possibly larger aggregates. In the flocculation settling range, the typical relationship of the settling velocity to the concentration is

$$W_s=k_1C^{\alpha} \tag{10}$$

Theoretically, α is 4/3, although the actual value typically varies between about 0.8 and 2 (Krone, 1962; Mehta, 1988b). The proportionality coefficient, k_1, can vary by an order of magnitude depending upon sediment composition and flow environment.

At concentrations in excess of C_2, the occurrence of an aggregate network hinders the upward transport of interstitial water. Consequently, W_s decreases with increasing C (Kynch, 1952) as indicated in Fig. 5. This is commonly termed hindered settling. The general expression for the settling velocity in the hindered settling region is

$$W_s=W_{so}[1-k_2(C-C_2)]^{\beta} \tag{11}$$

where W_{so} is the maximum settling velocity that corresponds to C_2, k_2 is the inverse of the concentration in excess of C_2 at which $W_s=0$ and theoretically β is 5. Although the settling velocity decreases at concentrations in excess of C_2, however, the settling flux, F_s, increases with C up to C_3 where it attains a peak value of F_{so}. This is due to the minuscule decrease of settling velocity between C_2 and C_3 in comparison with the increase of concentration. At values of C higher than C_3 the flux also decreases relatively rapidly with increasing C. At concentrations greater than C_4 there is negligible settling.

Fig. 6 shows an example of settling velocity data using Lake Okeechobee mud obtained in a 2 m tall settling column (Hwang, 1989). The relationship

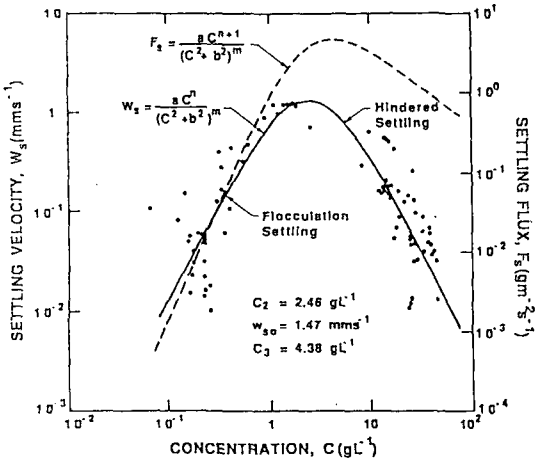

Fig. 6. Settling velocity data from a laboratory settling column experiment using sediment and fluid from Lake Okeechobee.

$$W_s=\frac{aC^m}{(C^2+b^2)^m} \tag{12}$$

which is modified from Wolanski *et al.* (1989), has been used to represent both flocculation settling and hindered settling, with a=33.38, b=2.54, n=1.83 and m=1.89. Note that the corresponding curve for the flux, F_s, is obtained by replacing n by n+1 in Eq. (4). Note further that the peak value of Ws is defined by

$$W_{so}=ab^n\ ^{2m}\frac{(2m/n-1)^{m\ n/2}}{(2m/n-1)^{1/2}} \tag{13}$$

and furthermore

$$C_2=\frac{b}{\left(\frac{2m}{n}-1\right)^{1/2}} \tag{14}$$

and

$$C_3=\frac{b}{\left(\frac{2m}{n+1}-1\right)^{1/2}} \tag{15}$$

3.4 Diffusive Flux

Suspended fine sediments increase the bulk density of suspension and lead to the vertically stratified structure of suspension density. This stratification due to bulk density variation alters the vertical fluid momentum and mass mixing characteristics. Bulk density, ρ_B, is related to suspension concentration, as

$$\rho_B=\rho_w+C\left(1-\frac{\rho_w}{\rho_s}\right) \tag{16}$$

where ρ_w and ρ_s are the water and sediment granular densities, respectively. When the bulk density increases upwards the stratification is stable and it becomes unstable when the density variation is reversed.

For turbulence under conditions of local equilibrium, the most obvious measure of stability (or mixing) is given by the gradient Richardson number

$$R_i=\frac{g\frac{\partial\rho_B}{\partial z}}{\rho_B\left(\frac{\partial u}{\partial z}\right)^2} \tag{17}$$

where g denotes gravity acceleration, u is the horizontal velocity magnitude, and z represents the vertically downward positive axis. Positive values of R_i indicate stable stratification, negative values denote unstable stratification, and $R_i=0$ corresponds to a neutral (non-stratified) condition. In the case of $R_i<0$, turbulent energy is increased and for $R_i>0$, buoyancy becomes negative, indicating that kinetic energy is lost. If a positive R_i becomes large enough, it leads to complete suppression of all turbulence.

Classical phenomenologically based forms for mass diffusivity in stratified flow are typically of the Munk and Anderson (1948) form as

$$K_z=\frac{K_n}{(1+\beta R_i)^\alpha} \tag{18}$$

where K_z and K_n are the vertical mass diffusivities for stratified and neutral flows, respectively, and α and β are generally non-negative empirical constants. Note that for positive α and β, increasing density gradient ($\partial\rho_B/\partial z$) leads to increasing R_i and consequently decreases K_z relative to K_n. It means that stratification acts to reduce diffusion by damping.

A plausible expression for the diffusivity under waves is given by Hwang and Wang (1982). They indicate, in the determination of diffusivity under

wave field, Prandtl's mixing theory may not be applicable due to the large scale of the wave motion. Emphasizing the dominant role of the vertical components of wave induced particle velocity in the diffusion process, they suggested the following expression for K_n:

$$K_n=\alpha_w\sigma H^2\frac{\sinh^2 k(h+z)}{2\sinh^2 kh} \tag{19}$$

where α_ω is a constant, H is wave height, σ is wave frequency, k is wave number, and h is water depth. Ross (1988) showed that this equation is a promising expression, based on energy dissipation consideration, for diffusivity under wave action. It should be noted that Eq. (19) is not applicable inside the wave boundary layer. Effects of the boundary layer next to the bed greatly increase the vertical mixing under waves due to the relatively large velocity gradients and shear (Neilson, 1979). However, diffusion in this layer is often neglected since it is very small (Maa, 1986). Outside the boundary layer, the velocity amplitude gradients increase with distance above the bottom to a maximum at the surface.

4. SIMULATION OF CONCENTRATION PROFILE

The vertical sediment transport model described previously was applied to Lake Okeechobee to examine the evolution of vertical suspension concentrations of fine sediment in wave-dominated environments, in general. The vertical transport model was originally developed by Ross (1988); however, the original model did not include the calculation of eroded or deposited bed depth and did not consider the effects of different degrees of wave action. Therefore, the model was modified for these purposes.

The vertical transport model solves Eq. (2) through a finite difference scheme, using boundary conditions specified by Eqs. (5) and (8), and the relationship between τ_s, ε_M and ρ_B given earlier. In order to run the model, the bed density profile in Fig. 4 was used. Through the least squares fit method, the expression for the variation of bulk density with bed depth was obtained using:

$$\rho_B=p_1\ \tanh[p_2(z+p_3)]+p_4 \tag{20}$$

where p_1, p_2, p_3 and p_4 are 0.087, 0.372, 5.8 and 1.087, respectively. The selected water depth was 4.6 m, as used by Gleason and Stone (1975). The settling velocity was obtained from Fig. 6 (Eq. (4)). In this case, the concentration C_1 below which settling was considered to be free was selected to be 0.1 g/L. A value of 0.5 was used for parameters α and β in Equation 18 and in Equation 19 the selected value of α_w for Lake Okeechobee was 1.56×10^{-2} The bed shear stress was computed from

$$\tau_b=\frac{1}{2}f_w\rho u_b^2 \tag{21}$$

where f_w is the wave friction factor, ρ is the fluid density and ub is the velocity amplitude at the bed obtained from linear wave theory. The parameter fw was selected to be 0.01 based on the work of Jonsson (1966); see Hwang (1989) for more details. The calculation of τ_b from u_b using Eq. (21), and the subsequent use of τ_b as the erosion forcing parameter implies quasi-steady conditions in which the rates of turbulence production and dissipation in the wave boundary layer are in equilibrium. This equilibrium assumption is therefore inherent in the present study.

Illustrations of simulated concentration profiles are shown in Figs. 7 and 8. The concentration profiles given in Fig. 7 pertain to the simulation of the Gleason and Stone (1975) field experiment. Since Gleason and Stone did not report wave conditions during their concentration measurements, storm waves of 0.9 m height and 4 sec. period were used to approximate extreme conditions in Lake Okeechobee. The simulation was started with a clear water column and a fluid mud layer near the bottom. The wave action was continued until the concentration reached 102 mg/L, with the aim to determine the corresponding erodible depth of the bed layer and the corresponding thickness of the fluid mud layer. For this purpose, it was necessary to specify a representative density (concentration) of the fluid mud layer, which was selected to be 39 g/L. As shown in Fig. 7, the 102 mg/L concentration occurred at about 11 hr after the beginning of wave action. At 11 hr, the model predicted 1.3 cm of bed erosion as compared to 2.3 mm of bed

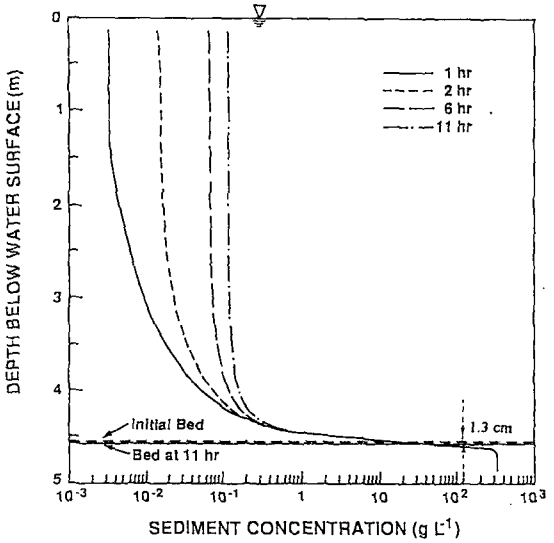

Fig. 7. Simulated evolution of suspension concentration profile due to 1 m high 6 sec waves in a 4.6 m deep water column.

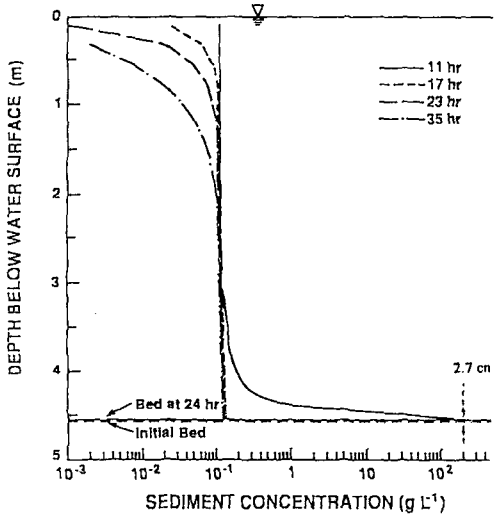

Fig. 8. Simulated settling of suspended sediment under no-wave condition.

erosion suggested by Gleason and Stone under the assumption of uniform water column concentration.

There is a qualitative agreement between the simulated results shown in Fig. 7 and the profile evolution under prototype conditions (profiles A, B, C) shown in Fig. 1 (Kemp and Wells, 1987). A noteworthy observation is that in both cases the concentration over the upper 80% of the water column is quite low, and that most of the sediment was concentrated over a relatively small height above the bed. Further entrainment of the lutocline was undoubtedly constrained by the submerged weight of the high concentration layer below the lutocline, and the lack of a strong mechanism for diffusion.

Fig. 8 represents the followup "post-storm" situation using the concentration profile at 11 hours (Fig. 7), assuming no wave action after this time. The profile at 35 hours resulted solely due to settling, indicating lower near-surface as well as near-bed concentrations than at 11 hours. At this stage, the redeposited bed depth was 2.7 cm. Eventually, of course, all of the material would settle provided the conditions remained calm. It is noteworthy that in reality the rate of reformation of the bed would most probably be slower than that implied from this simulation, because the density of newly formed bed will be lower than that of the initial bed used for the simulation shown in Fig. 7, the comparatively more settled initial deposit. Freshly deposited materials dewater and their density increases with time within hours (Parchure and Mehta, 1985). However, dewatering becomes slower in the presence of ongoing settling of the sediment from the upper water column (Sills and Elder, 1986).

5. ERODIBLE DEPTH

The erodible bed depth is dependent on the thickness and concentration of the overlying fluid mud zone. In order to examine this issue further it is essential to define this zone through physical reasoning. Here, an operational definition of the fluidized mud layer thickness, consistent with relatively easily and routinely obtained sedimentary data, is considered as follows (see Fig. 9).

Under conditions defined by settling of suspension in the absence of upward diffusion, or very weak diffusion, the lutocline can be represented by concentration C_3 in Fig. 5. The relevant argument for this statement is that at this elevation (C_3)

$$\frac{\partial F_s}{\partial C}=0 \tag{22}$$

By the chain rule Eq. (22) can be rewritten as

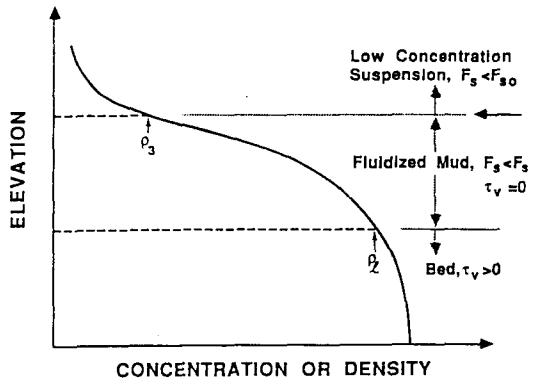

Fig. 9. An operational definition of fluid mud zone.

$$\frac{\partial F_s}{\partial C} = \frac{\partial F_s}{\partial z}\frac{\partial z}{\partial C} = \frac{\partial F_s/\partial z}{\partial C/\partial z} = 0 \qquad (23)$$

Eq. (23) implies that in order for $\partial F_s/\partial C = 0$, $\partial C/\partial z$, should approach infinity, which precisely represents the lutocline. Therefore, ρ_3 converted from C_3 can be considered to represent the upper level of the fluid zone. Below this level settling is hindered and the flux, F_s, decreases with depth. From Fig. 6 and Eq. (15), $C_3 = 4.38$ g/L, which yields $\rho_3 = 1.002$ g/cm^3, using $\rho_w = 1.0$ g/cm^3 and $\rho_s = 2.14$ g/cm^3. The rather low value of ρ_s is indicative of the high organics fraction in the sediment (Hwang, 1989).

The lower level of the fluid mud zone is conveniently defined here as the value of the bulk density, ρ_l, at and above which the substrate possesses a measurable shear strength, τ_v, as obtained from the standard vane shear test. In order to estimate ρ_l bottom cores were opened up and τ_v was measured at different depths below the mud surface. The bulk density of the mud was likewise measured at different depths. Fig. 10 shows the results based on an analysis of a number of cores from Lake Okeechobee. The data indicate a discernible correlation between τ_v and ρ_B. Extrapolation of the mean line yields a density of 1.065 g/cm^3 below which there is no strength; hence $\rho_l = 1.065$ g/cm^3 may be selected.

Given these values of ρ_3 and ρ_l, the density profile of Fig. 4 yields a 5 cm thick fluidized mud layer. Other density profiles from other sites in the lake showed a fluidized mud layer thickness up to 12 cm, which is consistent with the fluid zone thickness range of Gleason and Stone (1975).

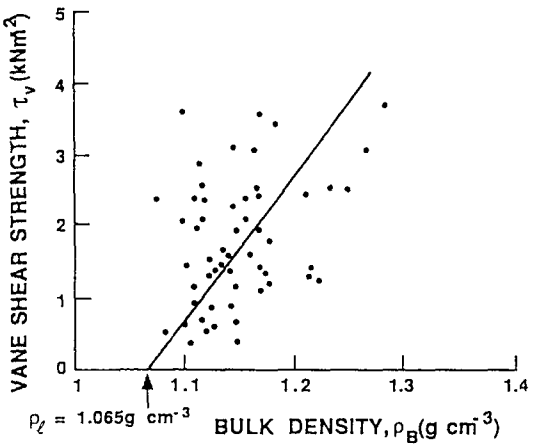

Fig. 10. Vane shear strength versus mud bulk density based on bottom core samples from Lake Okeechobee.

6. CONCLUDING REMARKS

The evolution of fine sediment concentration profiles and the corresponding eroded bed depth in a shallow lake have been examined assuming a purely wave determined flow environment. Simulation of the vertical sediment concentration profiles under storm wave action exhibited qualitative agreement with previous field observations of fine sediment concentration variation with depth. Characteristic features of the evolution process were the formation of a lutocline, the presence of a fluid mud layer near the bed and the existence of relatively low surficial concentrations. The concentration over the upper 80% of the water column was quite low, as most of the sediment was elevated over a relatively small distance above the bed. It is emphasized that based on these observations measurement of surface concentration alone can lead to an order of magnitude underestimation of the erodible bed depth. Accurate determination of the erodible bed depth depends upon an understanding of near-bed high concentration suspension dynamics.

Through an examination of the erodibility of mud by waves and the character of fluidized mud zone, an effort has been made to establish the connection between the erodible mud thickness due

to resuspension during storm wave action, and the fluidized mud zone thickness as identified from bottom cores. The actual thickness of this "active" mud surficial layer at a site will of course depend on the intensity and frequency of wave action, water depth and the thickness and character of the bottom mud. In Lake Okeechobee, the thickness of this active mud layer (fluidized mud thickness plus erodible bed thickness) appears to be on the order of 10 cm below the stationary mud-water interface.

The primary conclusion is that accurate measurement of instantaneous vertical concentration profiles is vitally important to studies of bottom sediment-induced turbidity, and in establishing the erodible thickness of the bed by wave action. Such profiling, when carried out effectively, can also yield valuable information on the microstructure of fine sediment suspensions, as has been demonstrated elsewhere (Kirby, 1986). Furthermore,it is essential to track the evolution of the near-bed suspended sediment load, since this highly non-Newtonian "slurry" is usually responsible for sedimentation problems in many episodic environments.

ACKNOWLEDGMENT

Support provided by the South Florida Water Management District, West Palm Beach, Florida through the Lake Okeechobee Phosphorus Dynamics Study is appreciated. Bottom coring work was carried out by Dr. Robert Kirby. Special thanks are extended to Dr. A.J. Mehta, for his valuable advice and suggestions throughout this study.

REFERENCES

Gleason, P.J., and Stone, P.A., 1975. Prehistoric trophic level status and possible cultural influences on the enrichment of Lake Okeechobee, *Unpublished Report*, South Florida Water Management District, West Palm Beach, Florida.

Hwang, K.-N., 1989. Erodibility of fine sediment in wave-dominated environment, *MS Thesis*, University of Florida, Gainesville, FL.

Hwang, P.A., and Wang, H., 1982. Wave kinematics and sediment suspension at wave breaking point, *Technical Report No. 13*, Department of Civil Engineering, University of Delaware, Newark, Delaware.

Jonsson, I.G., 1966. Wave boundary layer and friction factors, *Proceedings of the 10th Coastal Engineering Conference*, ASCE, Vol.1, pp. 127-148.

Kemp, G.P., and Wells, J.T., 1987. Observations of shallow-water waves over a fluid mud bottom: Implications to sediment transport, *Coastal Sediments '87*, ASCE, New York, pp. 363-378.

Kirby, R., 1986. Suspended fine cohesive sediment in the severn estuary and inner Bristol Channel, U.K., *Report ETSU-STP-4042*, Department of Atomic Energy, Harwell, United Kingdom.

Krone, R.B., 1962. Flume studies of the transport of sediment in estuarial shoaling process, *Final Report*, Hydraulic Engineering Laboratory and Sanitary Engineering Research Laboratory, University of California, Berkeley, California.

Kynch, G.J., 1952. A theory of sedimentation, *Transactions of the Faraday Society*, Vol. 48, pp. 166-176.

Lick, W., 1982. Entrainment, deposition and transport of fine-grained sediment in lakes, *Hydrobiologia*, Vol. 91, pp. 31-40.

Luettich, R.A., Jr., Harleman, D.R.F., and Somlyody, L., 1989. Suspended sediment concentration in a shallow lake, *Limmology and Oceanography*.

Maa, P.-Y., 1986. Erosion of soft muds by waves, *Ph.D. Dissertation*, University of Florida, Gainesville, Florida.

Maa, P.-Y., and Mehta, A.J., 1987. Mud erosion by waves: A laboratory study, *Continental Shelf Research*, Vol. 7, Nos. 11/12, pp. 1269-1284.

McCutcheon, S.C., 1983. Vertical mixing in models of stratified flow, *Proc. Conference on Frontiers in Hydraulic Engineering*, ASCE, pp. 15-20.

Mehta, A.J., 1988a. Laboratory studies on cohesive sediment deposition and erosion, *Physical Processes in Estuaries*, J. Dronkers and W. van Leussen, eds., Springer-Verlag, Berlin, pp. 427-445.

Mehta, A.J., 1988b. Cohesive sediments in estuarine environment, *Invited Contribution to AGU Chapman Conference*, Bahia Blanca, Argentina.

Munk, W.H., and Anderson, E.R., 1948. Notes on the theory of the thermocline, *Journal of Marline Research*, Vol. 1, pp. 276-295.

Neilson, P., 1979. Some basic concepts of wave sediment transport, *Paper No. 20*, Institute of Hydrodynamics and Hydraulic Engineering, Technical University of Denmark, Lyngby, Denmark.

Odd, N.M.V., and Rodger, J.G., 1986. An analysis of the behavior of fluid mud in estuaries, Rept. SR 85, Hydraulic Research, Wallingford, UK.

Parchure, T.M., and Mehta, A.J., 1985. Erosion of soft cohesive sediment deposits, *Journal of Hydraulic Engineering*, ASCE, Vol. 3, No. 10, pp. 1308-1326.

Richardson, J.F., and Zaki, W.N., 1954. The sedimentation of a suspension of uniform spheres under conditions of viscous flow, *Chemical Engineering Science*, Vol. 3, pp. 65-72.

Ross, M.A., 1988. Vertical structure of estuarine fine sediment suspensions, *Ph.D. Dissertation*, University of Florida, Gainesville, Florida.

Sills, G.C., and Elder, D.McG., 1986. The transition from

suspension to settling bed, *Estuarine Cohesive Sediment Dynamics*, A.J. Mehta ed., Springer-Verlag, Berlin, pp. 192-205.

Srinivas, R., 1989. Response of fine sediment-water interface to shear flow, *M.S. Thesis*, University of Florida, Gainesville, FL.

Wolanski, E., Aseda, T., and Imberger, J., 1989. Mixing across a lutocline, *Limnology and Oceanography*, Vol. 34, pp. 931-938.